AD A137 040 ELECTROCHEMICALLY MODULATED INFRARED SPECTROSCOPY (EMIRS) EXPERIMENTAL DETAILS(U) UTAH UNIV SALT LAKE CITY DEPT OF CHEMISTRY A BEWICK ET AL. 06 JAN 84 TR 18 1/1

UNCLASSIFIED N00014 83 K 0470 F/G 7/4 NL

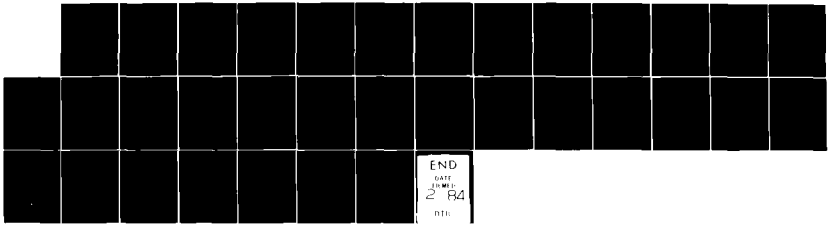

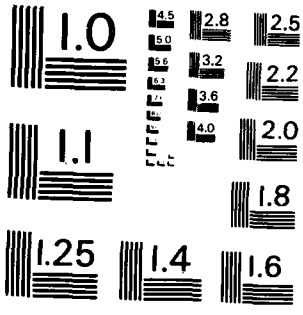

SECURITY CLASSIFICATION OF THIS PAGE (When Data Entered)

REPORT DOCUMENTATION PAGE		READ INSTRUCTIONS BEFORE COMPLETING FORM
1. REPORT NUMBER: 18	2. GOVT ACCESSION NO.	3. RECIPIENT'S CATALOG NUMBER
4. TITLE (and Subtitle): Electrochemically Modulated Infrared Spectroscopy (EMIRS) - Experimental Details		5. TYPE OF REPORT & PERIOD COVERED: Technical Report # 18
		6. PERFORMING ORG. REPORT NUMBER
7. AUTHOR(s): A. Bewick, B.S. Pons, J.W. Russell, K. Kunimatsu		8. CONTRACT OR GRANT NUMBER(s): N00014-83-K-0470
9. PERFORMING ORGANIZATION NAME AND ADDRESS: University of Utah, Department of Chemistry, Salt Lake City, UT 84112		10. PROGRAM ELEMENT, PROJECT, TASK AREA & WORK UNIT NUMBERS: Task No. NR 359-718
11. CONTROLLING OFFICE NAME AND ADDRESS: Office of Naval Research, Chemistry Program - Chemistry Code 472, Arlington, Virginia 22217		12. REPORT DATE: January 6, 1984
		13. NUMBER OF PAGES
14. MONITORING AGENCY NAME & ADDRESS (if different from Controlling Office)		15. SECURITY CLASS. (of this report): Unclassified
		15a. DECLASSIFICATION/DOWNGRADING SCHEDULE

16. DISTRIBUTION STATEMENT (of this Report)

This document has been approved for public release and sale; its distribution unlimited.

17. DISTRIBUTION STATEMENT (of the abstract entered in Block 20, if different from Report)

18. SUPPLEMENTARY NOTES

19. KEY WORDS (Continue on reverse side if necessary and identify by block number)

IR Spectroelectrochemistry

20. ABSTRACT (Continue on reverse side if necessary and identify by block number)

Electrochemically modulated infrared spectroscopy (EMIRS) has proven to be a highly sensitive in situ technique for the obtaining of vibrational spectra of species adsorbed on metal electrodes. This paper presents a description of the experimental details regarding the methods and equipment necessary for the EMIRS technique.

DD FORM 1473 EDITION OF 1 NOV 65 IS OBSOLETE S/N 0102-LF-014-6601

Unclassified

SECURITY CLASSIFICATION OF THIS PAGE (When Data Entered)

AD A137040

DTIC FILE COPY

ELECTE JAN 20 1984 A

84 01 17 120

OFFICE OF NAVAL RESEARCH

Contract N00014-83-K-0470

Task No. NR 359-718

TECHNICAL REPORT NO. 18

Electrochemically Modulated Infrared Spectroscopy (EMIRS) - Experimental Details

By

A. Bewick
K. Kunimatsu
B.S. Pons*
J.W. Russell

Prepared for Publication in

Journal of Electroanalytical Chemistry

University of Utah
Department of Chemistry
Salt Lake City, UT 84112

January 6, 1984

Electrochemically Moduleted Infrared Spectroscopy (EMIRS) - Experimental Details

A. Bewick*, K. Kunimatsu[1], B.S. Pons[2] and J.W. Russell[3].

*Department of Chemistry,
University of Southampton,
Southampton SO9 5NH
England.

[1]On leave from:
Research Institute for Catalysis,
Hokkaido University,
Sapporo, Japan.

[2]Present address:
Department of Chemistry,
University of Alberta,
Edmonton,
Canada.

[3]On leave from:
Department of Chemistry,
Oakland University,
Rochester,
Michigan 48063,
U.S.A.

A1

AC8206751

ABSTRACT

Electrochemically modulated infrared spectroscopy (EMIRS) has proven to be a highly sensitive in situ technique for the obtaining of vibrational spectra of species adsorbed on metal electrodes. This paper presents a description of the experimental details regarding the methods and equipment necessary for the EMIRS technique.

Introduction

Historically, the development of many major areas of electrochemistry has been greatly frustrated by the lack of the experimental means to obtain direct information on the identity and the molecular structure of species in the electrode/electrolyte solution interphase and on the orientation and bonding of such species to the electrode surface. The sense of frustration has been highlighted by the spectacular developments in high vacuum surface science brought about by the application of new spectroscopic methods which can, at best, be used only as ex-situ techniques in the electrochemical context. Thus the steady development of surface enhanced Raman spectroscopy, SERS, as an in situ electrochemical method has been particularly welcomed (1). It had always been assumed that the presence of an aqueous electrolyte solution would cause insuperable problems to the development of external reflectance infrared spectroscopy as an in-situ technique; the earlier, pioneering spirits had, therefore, directed their energies towards internal reflectance methods (2,3), which unfortunately provided scant reward for the experimental effort expended. During the past few years, however, an external reflectance technique, electrochemically modulated infrared spectroscopy (EMIRS), has been successfully demonstrated (4,5) and applied to a number of electrochemical systems (6-10). Subsequently, the range of external reflectance IR methods has been expanded with the development of a modified technique which

exploits the advantages of Fourier Transform Infrared Spectroscopy (11) and by the successful application to electrochemical systems of a polarisation modulation method, IRRAS, originally developed to study adsorption of gases on metal surfaces (12). In this paper, we present a detailed discussion of the equipment and the experimental methods developed for the EMIRS technique.

Reflection of electromagnetic radiation at a metal surface

Two phenomena associated with the optics of the reflection of electromagnetic radiation from a highly reflecting metal surface are pertinent to the present discussion. For other than normal incidence, the effective intensity of the radiation very close to the surface is different for the p-polarised and s-polarised states. There is a 180° phase change on reflection at a metal surface at all angles of incidence for s-polarised radiation, which has its electric vector tangential to the surface, and since the reflection coefficient is close to unity, the resultant amplitude of the electric vector at the surface is essentially zero. Thus s-polarised infrared radiation does not interact with vibrating dipoles near the surface, i.e. it is inactive in the detection of adsorbed species. Consequently, only p-polarised radiation, which has its electric vector in the plane of incidence, is effective for studies at metal surfaces. This leads to an additional selection rule, the surface selection rule (13),

defining those normal modes of a molecule sitting on a metal surface able to show IR activity, i.e. only those vibrational modes having a non-zero component of the dipole derivative perpendicular to the surface, $(\partial\mu/\partial Q)_{\perp}$, are able to interact with the IR radiation. A useful consequence of this is that the relative intensities of the absorption bands shown by an adsorbed molecule will vary as its orientation with respect to the surface is changed. This sensitivity towards orientation is a very valuable feature of the EMIRS method.

There is also a strong angular dependence of the interaction of p-polarised radiation with an adsorbed layer. As the angle of incidence is increased away from the normal, the interaction rises sharply, peaks near grazing incidence and then declines to zero. Thus high angles of incidence confer greatly enhanced sensitivity to reflection measurements but other optical considerations, particularly those encountered in coupling an electrochemical cell to the IR radiation, often preclude the use of very high angles.

Description of the EMIRS technique

EMIRS is essentially a direct development of the specular reflectance technique (14) previously used in the UV-visible spectral region. While UV-visible spectra have been used to identify electrochemically produced species, extension into the region of vibrational spectra offers the possibility for obtaining structural as well as identity information. It is to be expected that infrared spectra of adsorbates in electrochemical systems will provide evidence for molecular orientations with respect to the electrode surface and probe

the strengths of interactions between adsorbates-substrates, adsorbates-adsorbates, and adsorbates-solution species. As in the UV-visible technique, radiation is specularly reflected from a polished electrode surface while the electrode potential is modulated with a square waveform. Amplification of only that component of the optical signal in-phase with the potential modulation increases the sensitivity to the level adequate for detection of infrared bands of submonolayer quantities of adsorbates (typically, measurement of absorbance changes smaller than 10^{-4} is required). For infrared spectroscopy of strongly IR absorbing aqueous solutions, very different requirements are placed on the design of the cell than for UV-visible spectroscopy. A thin layer spectroelectrochemical cell suitable for use with aqueous solutions throughout the infrared region has been developed and is described in a subsequent section.

The signal observed in an EMIRS experiment is proportional to the difference in the intensity of the radiation received by the detector while the electrode is alternately at one of two fixed potentials defined by the square wave modulation. Although this intensity difference is represented in EMIRS spectra as a reflectivity difference, ΔR, it may originate from several sources including the electroreflectance effect as well as changes in the amount of absorbed species in the inner region of the electrical double layer or in the layer of solution traversed by the IR beam. These latter sources are likely to be the subject of most EMIRS studies. In such studies, EMIRS spectra correspond to difference spectra between species present at the two selected electrode potentials. For ease of comparison with

usual infrared spectra, EMIRS results are presented as plots of $\Delta R/R$ vs wavenumber. This $\Delta R/R$ ratio removes the wavenumber dependence of instrumental energy throughput, detector sensitivity, and electronic response. A single beam spectrometer acts as a nearly perfect pseudo-double beam spectrometer since the identical optical path is followed by "beams" separated temporally but not spatially at the modulation frequency. Values of $\Delta R/R$ are proportional to the difference of two absorbance values.

Since EMIRS spectra are difference spectra, it is important to recognise the possible origins for various spectral features which may occur and to be aware of the limitations placed upon spectral observations and/or interpretations. If ΔR is defined as the reflectivity at the more positive potential, R_a, minus the reflectivity at the more negative potential, R_c, the correspondence between infrared features for species present at these potentials and the EMIRS difference spectrum is shown for the most likely possibilities in Figure 1. Figure 1a illustrates how the electroreflectance effect could produce a non-zero and possibly non-flat spectral baseline. In Figure 1b the absorption band for a species present only at one of the two selected electrode potentials is shown as positive or negative depending upon whether the species occurs at the negative or the positive potential respectively. A change in intensity of an infrared band with a change in potential might result from: (1) a dependence upon potential of the amount of species present, (2) a potential dependence of the infrared oscillator strength, or (3) a dependence of the orientation of the species with respect to the electrode

surface upon electrode potential. This last case arises due to the surface selection rule discussed in the previous section. For species close to the electrode surface compared with the wavelength of the radiation, only vibrational modes with non-zero surface normal dipole derivative components, $(\partial\mu/\partial Q)_\perp$, can absorb energy from the infrared beam. Since the strength of such absorption is proportional to $(\partial\mu/\partial Q)^2_\perp$, a reorientation of species with respect to the electrode surface will produce a change in band intensity. Bisignate EMIRS bands could arise if the band position were potential dependent (Figure 1d) or if the band shape were potential dependent in a way to move intensity from one side to the other (Figure 1e). A symmetrical change in band shape could produce a more complicated trisignate feature (Figure 1f). To date examples of the cases shown in Figures 1a, 1b, 1c and 1d have been observed and will be illustrated below. A disadvantage of the difference spectrum method is that if combinations of the above limiting cases occur the true origin of an EMIRS band might be obscured. In the worse case the difference might be too small to detect even for strong infrared features. In principle, however, integration of an EMIRS spectrum obtained with a sufficiently small modulation amplitude will yield the true absorption spectrum but it will be shifted by the unknown constant of integration and the amplitude will, in some cases, be scaled by an unknown factor.

The detection by EMIRS of submonolayer amounts of adsorbed species requires very high sensitivity but it is encouraging to note that nature is considerably more benevolent than would be

expected at first sight. Fig.2 shows the absorbance versus thickness curves for a layer of water in contact with a platinum electrode calculated at the wavelength of the maximum absorption of the OH stretch in two different ways: firstly, by a simple minded application of Beers Law, curve (a), and secondly, by a rigorous application of the Fresnel reflectance equation, curve (b). It can be seen from these curves that the energy transmitted through a thin layer of aqueous solution as is used in the EMIRS cell, about 1 μ thick, is considerably greater than expected Beers Law and, conversely, the absorbance of a layer of molec dimensions, such as a layer of adsorbed molecules, is several fold greater than predicted by Beers Law. Thus, in an EMIRS experiment, R is larger and ΔR is several times greater, than might be expected; a very useful circumstance as befits a descendant of Mohammed (15).

The major objective determining the design of spectrometer and cell is to achieve the best possible detectivity in terms of ΔR/R. This means aiming for the highest possible throughput of energy which has been reflected from the electrode surface. Since resolution is not a major problem, bands of less than 10 cm^{-1} half width are unlikely to be encountered, a spectrometer of relatively short focal length will suffice. It is also appropriate to overrun the IR source to give higher output at the expense of lifetime.

Spectroelectrochemical Cell

The design of a three electrode spectroelectrochemical cell is shown in Figure 3. The working electrode, consisting of a 5-10 mm diameter flat disc, is sealed in a glass tube extension on a syringe plunger or is attached to a copper rod covered by a Kel-F outer sleeve to permit electrical contact with the solution only by the front surface. This electrode is inserted through the barrel of the syringe which makes up the back of the cell body. If any appropriate glass is not availeble for sealing a particular metal, the electrode may be attached with epoxy. These electrodes are ground flat and polished before each use with a slurry containing in successive order 1.0, 0.3, and 0.05 micron alumina in water. The Luggin capillary probe for the reference electrode extends parallel to the working electrode support rod to within one millimeter of the cell window. A wire loop near the centre of the cell through which the working electrode is inserted forms the counter electrode.

Two designs for the cell window have been used. Flat 1.5 mm thick silica, SiO_2, or silicon, Si, windows are sealed in appropriate ground glass joints, or a calcium fluoride, CaF_2, window is prepared from a 6 mm thick blank glued with epoxy to a glass joint. Although silicon windows of 1.5 mm thickness are useful to low wavenumber and are not attacked by dilute acid solutions, they have two serious limitations: (1) silicon is opaque to visible light which prevents the observation of the source image on the electrode

during cell alignment and (2) the high refractive index of the silicon produces high reflection losses for angles of incidence away from the Brewster angle of 74 degrees. Thus, if the window could be illuminated at this angle of incidence, the unwanted perpendicularly polarised component would be totally reflected and the parallel polarised component would be completely transmitted. In practice, such a well defined angle of incidence cannot be achieved without a well collimated beam and, moreover, the Brewster angle cannot be achieved simultaneously for the air/window interface and for the solution/window interface which is encountered following reflection from the electrode surface. The fore-optics design shown in figure 5 does not collimate the beam and typically it was adjusted to give an angle of incidence of 60° for a cone of radiation with a spread of $\pm 12^{\circ}$. Thus, even with use of a subsequent polariser to reject the perpendicular component, approximately half of the radiation reaching the detector comes from a window rather than the electrode. This window radiation is not modulated, however, and since infrared spectrometers are detector noise limited it does not contribute significantly to the noise level. However, it does represent a reduction in the percentage of the source intensity useful for spectroscopy. Silica windows avoid the problems of visible opaqueness and high reflection losses. Using these windows the images from the electrode and from the window can be separated

on the entrance slit such that only radiation reflected from the electrode reaches the detector. Silica is, however, limited to use at wavenumbers above 2300 cm^{-1}. The calcium fluoride windows are prepared with 65° bevelled edges to avoid reflection losses at the air window interface by using a zero degree angle of incidence with the window. The 65° angle for calcium fluoride was selected as the highest angle to avoid total internal reflection at the window solution interface when using aqueous acid solutions. The disadvantages of calcium fluoride are its small but finite water solubility and the need to attach windows with epoxy which is softened after a few days by acid solutions.

The working electrode is positioned snugly against the window and rotated to produce the highest signal for electrode reflected light. In this orientation average film thickness between the window and electrode of a few microns are obtained, e.g. for one particular electrode window combination, the intensity of the water fundamental modes was used to determine an average film thickness of two microns. These average film thicknesses represent wedge shaped layers since with the cell design of Figure 3 the possibility of the electrode surface being closely parallel to the cell window surface is very low. In none of the background reflectivity curves run during each experiment have the interference effects expected for a film with parallel surfaces ever been observed. The thin solution layer necessary for infrared transmission through aqueous solutions possesses potential electrochemical complications. Transportation of species by diffusion from bulk solution to the film between the electrode and window may be greatly restricted. With the electrode

positioned against the window, diffusion of CO from a bulk solution saturated with CO(g) has been shown to take times of the order of one hour to produce saturation coverage of CO(ad) on a platinum electrode (16). The thin film may also place severe restrictions on potential modulation rates particularly with the reference electrode positioned as in Figure 3. Figure 4 shows the CO stretching mode as a function of modulation frequency for CO_{ads} at saturetion coverage on a Pt electrode. The decrease in band intensity as the modulation frequency increases is interpreted as showing a reduction in the effective potential modulation range, although all spectra were obtained with a nominal range of 50-450 mV(NHE) set on the potentiostat. However, slow response of the electrode potential has rarely been found to be a serious problem; it is good practice to monitor the current/time transients caused by the modulation in order to estimate the response time and to check the detailed shape of the linear sweep voltammogram.

EMIRS Spectrometer Design

EMIRS spectra have been obtained using three different spectrometers. Original spectra were obtained on a 1/4 meter f/8 grating spectrometer used to demonstrate the feasibility of obtaining useful infrared spectra from electrochemical systems (4,5). Once the success of EMIRS had been established a high energy throughput spectrometer optimised for EMIRS was designed. This instrument is described below. Lower (1%)

resolution EMIRS spectra have also been recorded on a non-grating, variable filter spectrometer used at the University of Minnesota for IRRAS studies (11,16). The new EMIRS spectrometer was assembled by Anaspec Ltd. utilizing a 1/2 meter f/4 monochromator. The monochromator has a three position grating mount equipped with 84 x 84 mm Jarrell-Ash echelle gratings with the following specifications of grooves/mm and blaze positions: 150/mm (4μ), 50/mm (10μ), and 40/mm (22μ).

The optical layout for the monochromator sampling chamber fore-optics, and detector chamber optics is shown in Figure 5. A Nernst filament operated at a temperature of approximately 2300°C serves as the source. At this above-rating temperature filaments last several months in continuous operation. All spherical mirrors (M_1, M_2, and M_4) are used at low off-axis angles to minimize aberrations. Mirrors M_3 and M_5 used at large angles of incidence are plane mirrors. With the Pye IR50 pneumatic detector, a Pfund mirror design is used to image the exit slit on the detector window. With the HgCdTe photoconductive detector a KBr lens (40 mm diameter, 30 mm focal length) focussed the radiation from the monochromator upon the detector. Even though the detector chamber is purged with a slow flow of dry air, the lens mount is fitted with a heating element to keep the temperature of the lens above 30°C and prevent condensation during periods the purge is broken to reposition the detector or switch transmission filters. The chopper, C, is used to produce an 8.5 Hz signal for background, R, spectra but is positioned on an open quadrant when potential modulated, ΔR, spectra are being measured. F is an eight position filter wheel used for order sorting and P a silicon reflection polarizer or a gold grid transmission polarizer. The

polarizer is used to remove the perpendicularly polarized component of the radiation incident upon the electrode since this component contains no spectral information as discussed above. The main monochromator chamber and detector chambers are kept under constant purge by a slow stream of dry air. When spectral regions containing strong atmospheric absorptions are studied the sample chamber can also be purged. The alignment procedure for the cell and fore-optics is given below in the discussion of experimental procedures.

A block diagram of the components used for electrode potential modulation and signal processing is shown in Figure 6. The height of the potential step used for the square wave modulation of the electrode is set on the waveform generator and added to the base potential set on the potentiostat. Using the sign conventions of Figure 1, the negative potential is set on the potentiostat and the potential step required to give the positive potential is set on the waveform generator. The signal processing and monochromator control by the computer are described under experimental procedures.

Experimental Procedures

The procedures for cleaning the cell, polishing the electrode, and preparing samples have been previously described (6). The cell is positioned such that the source image, demagnified by a factor of two, is focussed upon the surface of the electrode. Since the source image at the electrode is higher than the circular electrode, vertical adjustment is made to position the electrode in the centre of the image. Tilt adjustments are made in order to collect

all the light reflected from the cell on mirror M_2 which forms a remagnified 1:1 image of the source at the chopper position. With the image from the electrode at the vertical centre of the entrance slit and all cell radiation collected by mirror M_2, the rotation of mirror M_2 about its vertical axis is adjusted to produce a maximum signal at the detector from the electrode with the chopper on.

The proper grating for the spectal region of interest is selected using the manual grating switching control and the appropriate transmission filter positioned after the exit slit. The spectral region to be scanned and the number of data points to be used to cover this region are set on the computer. Two background scans are run to determine the electrode reflectivity curve, R. During the first scan the electrode is withdrawn from the window and during the second positioned against the window. The difference in energy between these two scans is the background R curve from the electrode for the chosen spectral range. During the background scans the chopper is on and the electrode can be held at any potential or even modulated since the ΔR curves produced during potential modulation are orders of magnitude weaker than the R curve. For background and sample scans the monochromator is moved by uniform wavenumber increments by the computer giving the grating drive stepping motor the appropriate number of pulses. After each increment a delay of between one half and one second, as set on the computer, occurs before a reading is made of the output signal of the lock-in amplifier

to permit damping out of noise produced by stepping the grating. Data are recorded during monochromator movement to both higher and lower wavenumbers with appropriate corrections made upon each grating direction reversal to compensate for backlash in the gears. For background scans the lock-in reference signal may either be taken from a photocell mounted opposite a visible lamp at a position cut by the chopper blades or by using the preamplifier output for both signal and reference inputs.

Sample (ΔR) scans over the chosen spectral region are made with the chopper positioned in the open position and the desired potential modulation applied to the electrode. For such scans the lock-in reference is taken from the waveform generator and is phase adjusted for delays produced by detector response. The controlling computer program was written to permit display of the ΔR spectrum on the CRT after a preset number of scans. Data for each spectral element is collected in one computer memory location as the sum of the detector signals for that element from all scans. If an adequate signal-to-noise ratio has been achieved, the ΔR spectrum may be ratioed by the R spectrum to give a $\Delta R/R$ spectral plot. If the ΔR signal-to-noise ratio is still low, additional scans may be taken before displaying again on the CRT. R, ΔR, and/or $\Delta R/R$ plots may all be plotted on the hard copy plotter and/or stored on a floppy disk.

The detectivity of the system described depends, of course, on the chosen wavelength range and on the nature of the electrolyte. In regions of good energy throughput, bands with $\Delta R/R$ values as low as 10^{-6} can be detected.

Examples of EMIRS spectra

The EMIRS method is being used to investigate the nature of the adsorbed intermediates formed during the electrocatalytic oxidation of organic fuels (8 - 10). Figure 7 shows a spectrum obtained at a polycrystalline Pt electrode in 0.5M methanol + 1M H_2SO_4 when the electrode potential was modulated between +50 mV and +450 (NHE). The observed features are due to adsorbed CO which was shown to be the primary electrode poison for the electrocatalytic oxidation of methanol on platinum (8). The single-sided band at 1850 cm^{-1} is an example of a Figure 1c type band. The positive sign for $\Delta R/R$ indicates a species with stronger infrared absorption at the less positive potential (50 mV) than at the more positive potential (450 mV). The intensity of this band decreases as the electrode is made more positive and this is attributed to a decrease in the amount of adsorbed CO occupying multibonded sites, most likely three-fold sites. Early assignment of the bisignate EMIRS band at 2075 cm^{-1} as a Figure 1d example of a band which shifts position with a change in electrode potential has been firmly established by direct measurement of the infrared band at different electrode potentials using IRRAS (12,16). The IRRAS spectra showed this band, which is assigned to a CO molecule adsorbed linearly above a platinum atom, to shift linearly to a higher wavenumber, whilst retaining constant intensity and band shape, as the electrode potential is made more positive. The shift has been attributed to the effects of changes in the occupancy of the π^* antibonding orbital with changing availability of electrons.

An example illustrating both the electroreflectance effect (Figure 1a) and a species present at only one of the potentials used for modulation (Figure 1b) is given in Figure 8. This figure shows the spectral region around 5000 cm^{-1} where combination bands of H_2O and of HDO occur. The sample is 1M sulphuric acid in water with isotopic composition: H_2O (11%), HDO (44%), and D_2O (45%). The dominant features observed are $\nu_2+\nu_3$ of HDO at 2.04μ and $\nu_2+\nu_3$ of H_2O at 1.93μ. Spectra are shown for a series of experiments using modulation with a constant lower potential of 50 mV and several higher potentials. At +50 mV the polycrystalline platinum electrode is covered with adsorbed hydrogen. The upper limits were chosen to correspond to potentials at which progressive quantities of hydrogen have been desorbed through oxidation. If the electrode potential modulation spans the desorption peak for weakly bound hydrogen, infrared bands due to water vibrational modes are observed. Potential modulation spanning the second desorption peak produces a shift in the baseline to negative $\Delta R/R$ values. These results have been interpreted (6,7) in terms of a strong interaction between weakly adsorbed hydrogen atoms and a water layer containing mainly dimer units but with these units also bonded back to the bulk water. There appears to be no interaction between the water and the strongly bound hydrogen; the formation of this species simply produces a large increase in reflectivity which shows up as a smooth, negative baseline shift in figure 8. Thus adsorption/desorption of weakly adsorbed hydrogen results in Figure 1b type bands due to oriented water units hydrogen bonded to the adsorbed hydrogen atoms, while adsorption/desorption of strongly bound hydrogen produces a Figure 1a electroreflectance effect indicative of an increase

in conduction electrons when the species is formed.

Figure 9 shows the C=C and C≡N stretching bands for acrylonitrile adsorbed from a 0.1M C_2H_3N + 1M H_2SO_4 solution on a polycrystalline gold electrode. The fine structure on the C=C band at 1520 cm^{-1} is believed to be noise resulting from the much lower signal-to-noise ratio in this region of strong water absorption. The positive sign of $\Delta R/R$ for the two bands indicates stronger infrared absorption at the less positive potential. Since acrylonitrile is thought to be adsorbed on gold at both potentials this change in intensity of infrared adsorption may be an example of a change in oscillator strength produced by a change in electrode potential. The fact that both the C=C and C≡N stretching modes are strongly shifted towards lower wavenumbers from their respective values found for non-adsorbed molecules in dilute solution is taken as evidence for a molecular orientation parallel to the electrode surface (17). Thus the appearance of these modes on the spectra is an apparent violation of the surface selection rule. There are several alternative explanations for this. The normal mode motions of the atoms will be different for acrylonitrile in the adsorbed state; the C=C and C≡N vibrations will involve some motion of these atoms perpendicular to the surface and thus a dipole change perpendicular to the surface is likely. Additionally, the surface normal dipole induced by the static electrical field at the electrode surface would be espected to possess an oscillatory component in phase with the molecular vibrations.

Acknowledgement

Support for this work from the Office of Naval Research, Washington and the SERC is gratefully acknowledged.

References

1. Surface Enhanced Raman Scattering, Ed. R.K. Chang and T.E. Furtak, Plenum, New York, 1982.
2. H.B. Mark, B.S. Pons, Anal. Chem., 1966, 38, 119.
3. A.H. Reed and E. Yeager, Electrochim. Acta, 1970, 15, 1345.
4. A. Bewick, K. Kunimatsu, and B.S. Pons, Electrochim. Acta, 1980, 25, 465.
5. A. Bewick and K. Kunimatsu, Surf. Sci., 1980, 101, 131.
6. A. Bewick and J.W. Russell, J. Electroanal. Chem., 1982, 132, 329.
7. A. Bewick and J.W. Russell, J. Electroanal. Chem., in press.
8. B. Beden, C. Lamy, A. Bewick and K. Kunimatsu, J. Electroanal. Chem., 1981, 121, 343.
9. B. Beden, A. Bewick, K. Kunimatsu and C. Lamy, J. Electroanal. Chem., in press.
10. B. Beden, A. Bewick, M. Razaq and J. Weber, J. Electroanal. Chem., in press.
11. T. Davidson, S. Pons, A. Bewick and P.P. Schmidt, J. Electroanal. Chem., 1981, 125, 237.
12. J.W. Russell, J. Overend, K. Scanlon, M.W. Severson, and A. Bewick, J. Phys. Chem., in press.
13. R.M. Hexter and M.C. Albrecht, Spectrochim. Acta, Part A, 1978, 35, 233.
14. A.W.B. Aylmer-Kelly, A. Bewick, P.R. Cantrill, and A.M. Tuxford, Discuss. Faraday Soc., 1973, 56, 96.
15. EMIR - a descendat of Mohammed, Oxford English Dictionary.
16. J.W. Russell, J. Overend, K. Scanlon, M.W. Severson and A. Bewick, J. Phys. Chem., submitted.
17. A. Bewick and C. Gibilaro, to be published.

FIGURE LEGENDS

1. Examples of possible IR reflectance spectra and the corresponding EMIRS difference spectra. The spectra at the two different potentials are distinguished by the full lines and the dashed lines and the difference spectrum is plotted as a dotted/dashed line.

2. The absorption of IR radiation by a water layer in contact with a platinum mirror electrode calculated at the absorption maximum of the O-H stretch band according to (a) Beer's law and (b) the Fresnel reflectance equations.

3. Schematic diagram of the cell used for the EMIRS experiments.

4. EMIRS difference spectrum for $(CO)_{ads}$ on Pt; modulation frequency (a) 10 Hz, (b) 50 Hz, (c) 200 Hz, (d) 500 Hz, and (e) 1000 Hz.

5. Schematic diagram of the optics of the EMIRS spectrometer.

6. Block diagram of the complete spectrometer system.

7. Spectrum from a Pt electrode in 0.5M CH_3OH/1M H_2SO_4; modulation from +50 mV to +450 mV (NHE)

8. EMIRS spectra in the $\nu_1 + \nu_3$ region for HDO from a Pt electrode in 1M H_2SO_4 (50% D); modulation (a) 50-100mV, (b) 50-200 mV, (c) 50-250mV, (d) 50-450mV.

9. EMIRS spectra of acrylonitrile adsorbed on an Au electrode in 0.05M acrylonitrile/ 1M H_2SO_4; modulation 50-1000mV.

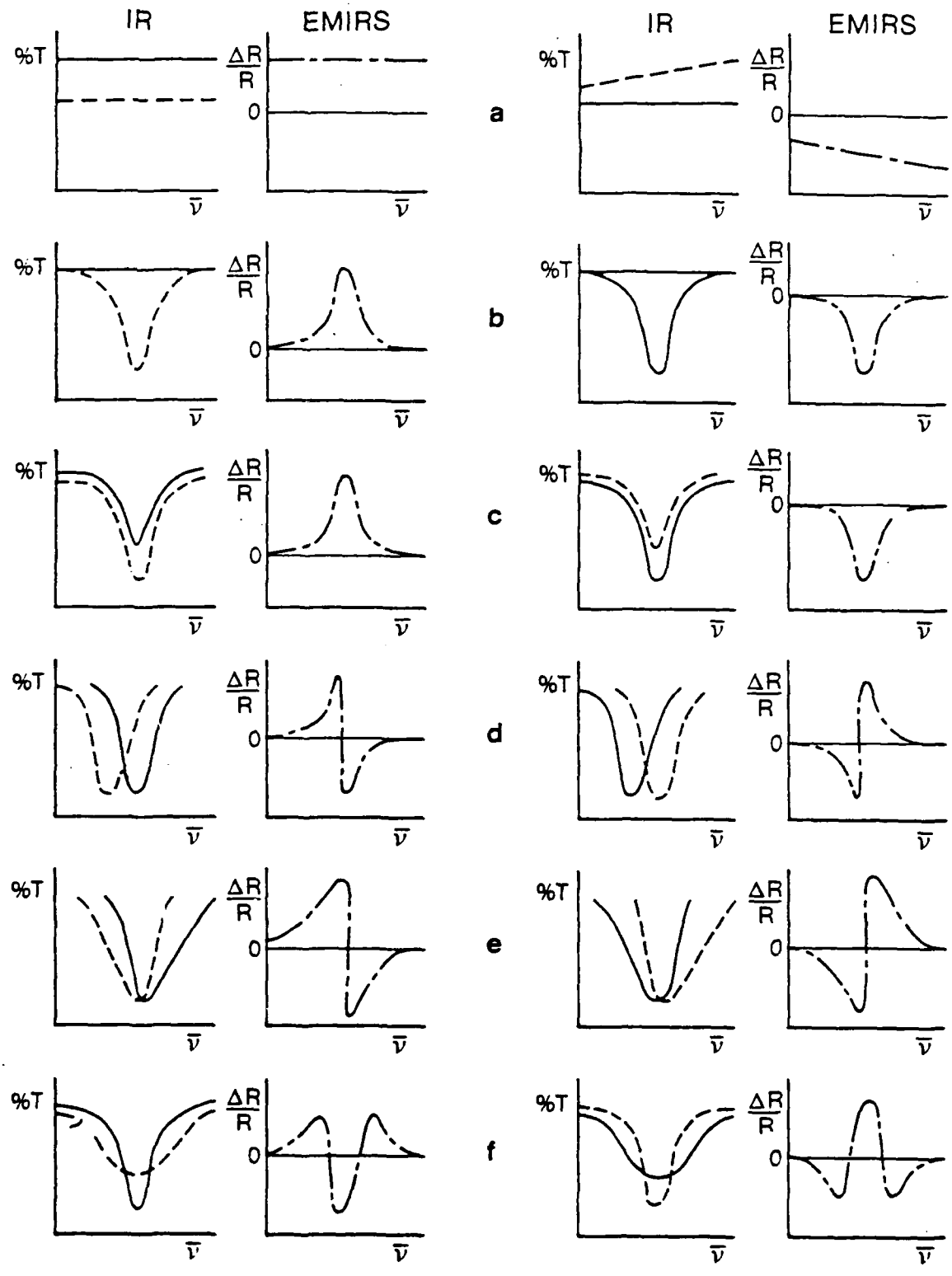
IR
EMIRS
IR
EMIRS
%T
ΔR/R
0
ν̄
a
b
c
d
e
f

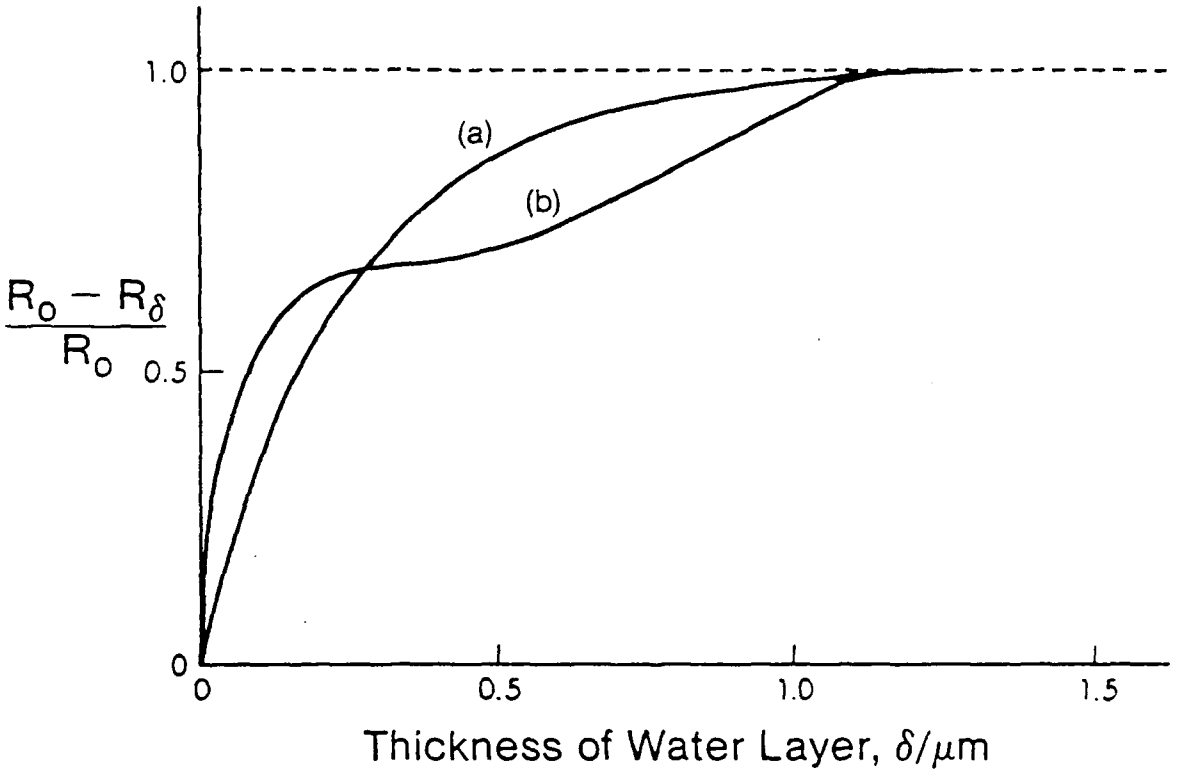
1.0
(a)
(b)
$\frac{R_o - R_\delta}{R_o}$
0.5
0
0
0.5
1.0
1.5
Thickness of Water Layer, $\delta/\mu m$

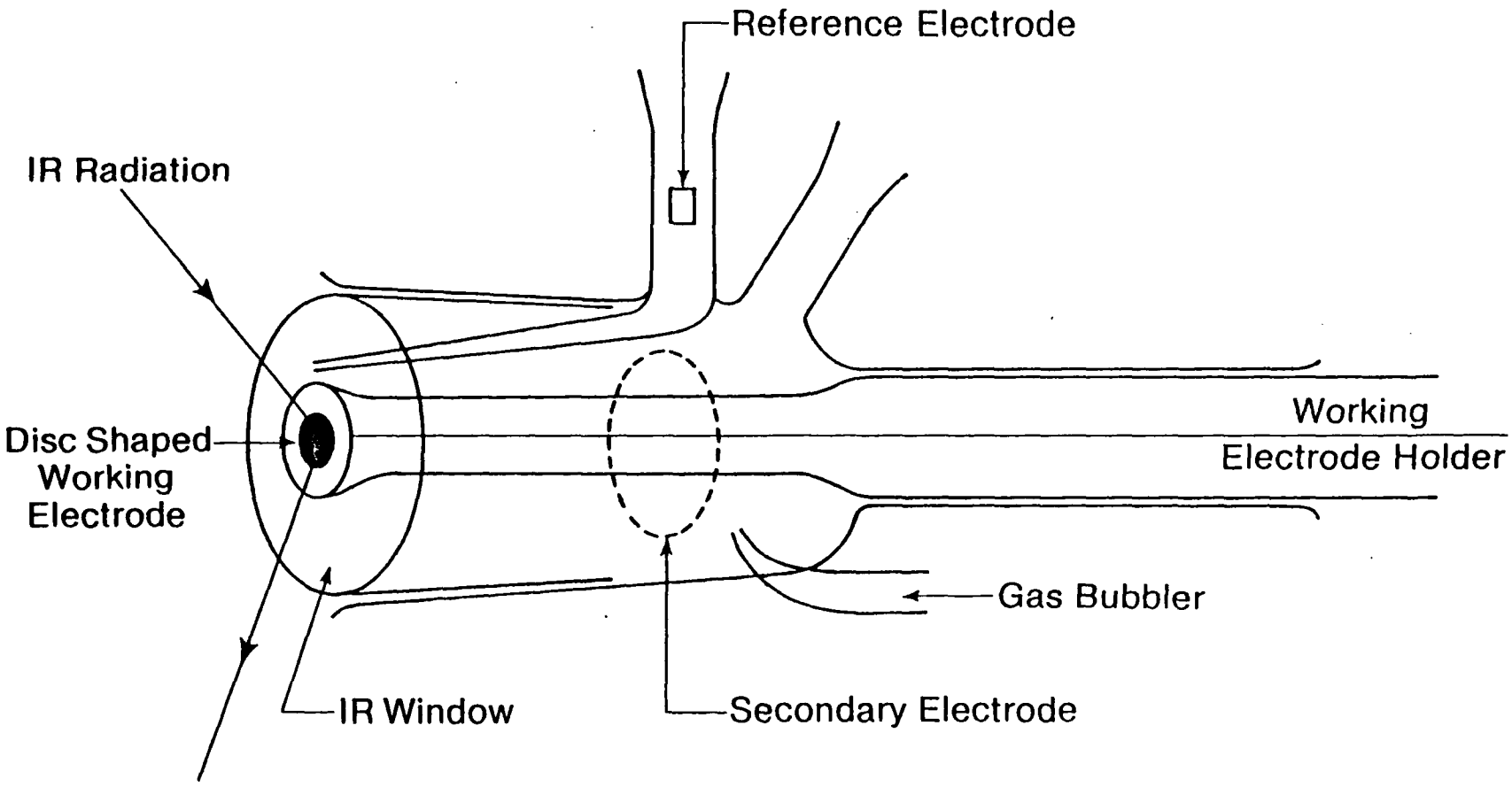

SCHEMATIC DIAGRAM OF ELECTROCHEMICAL INFRARED CELL

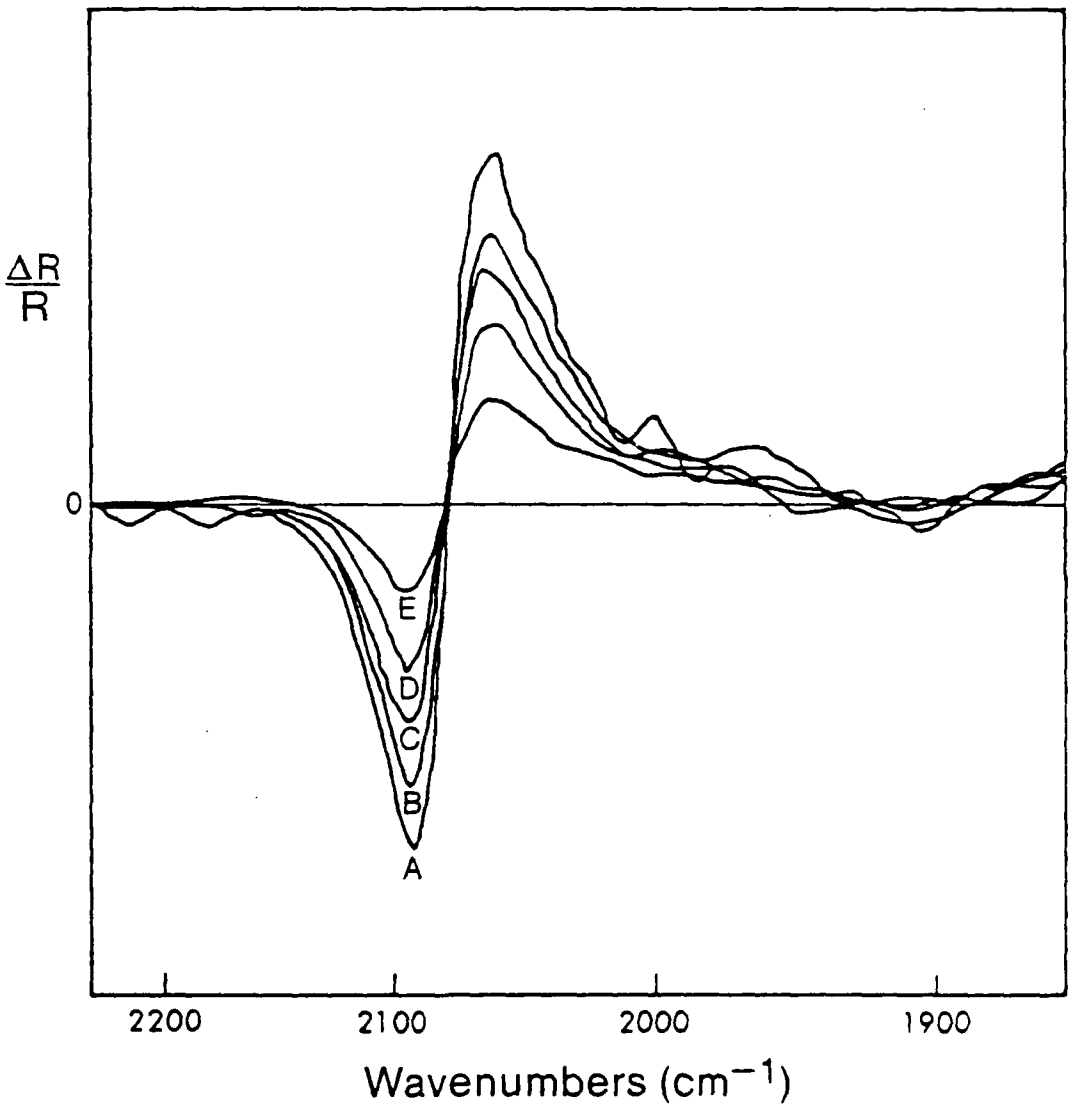
ΔR/R
0
E
D
C
B
A
2200
2100
2000
1900
Wavenumbers (cm⁻¹)

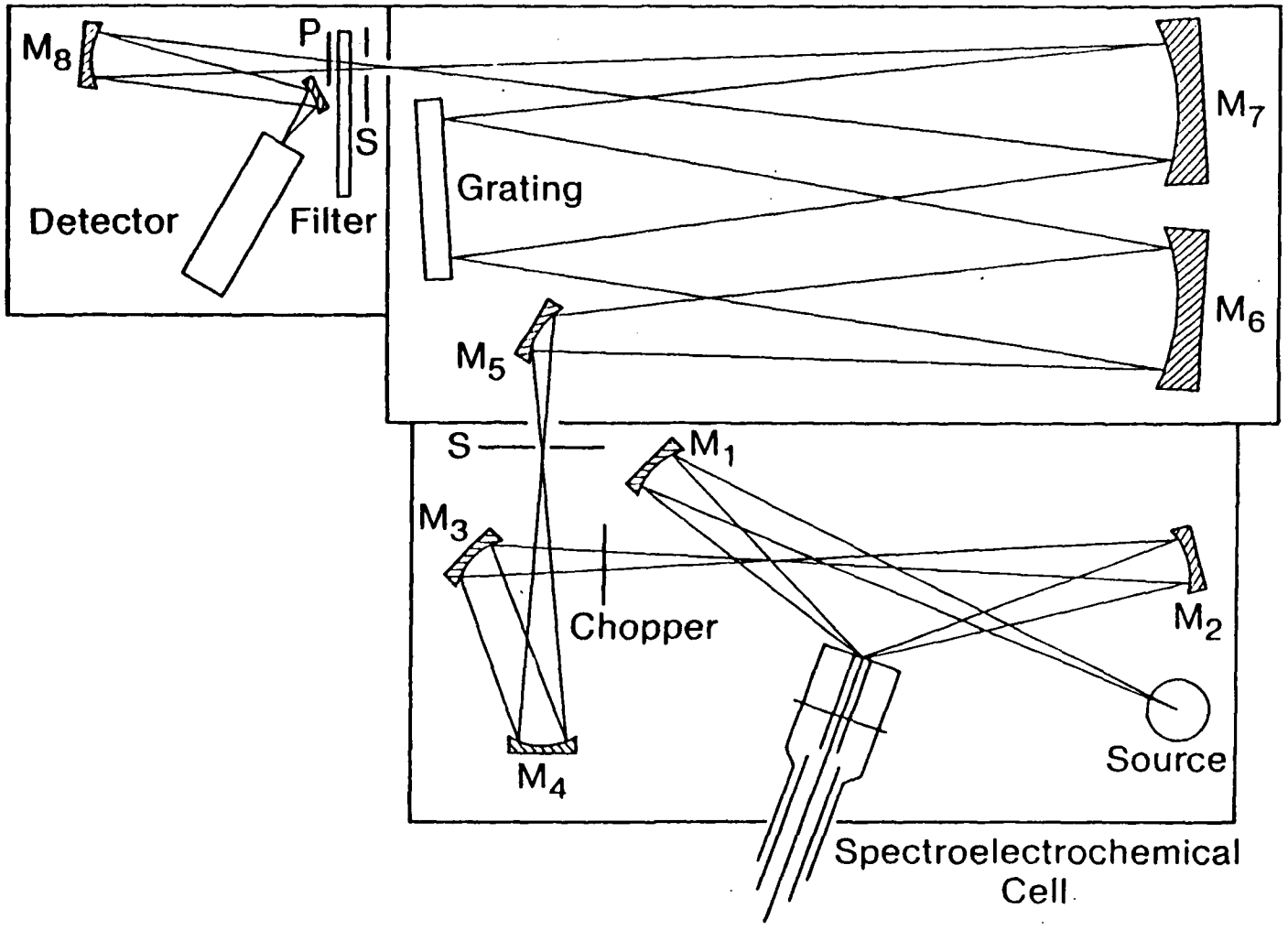
M8
P
S
Detector
Filter
Grating
M7
M6
M5
S
M1
M3
Chopper
M2
M4
Source
Spectroelectrochemical
Cell

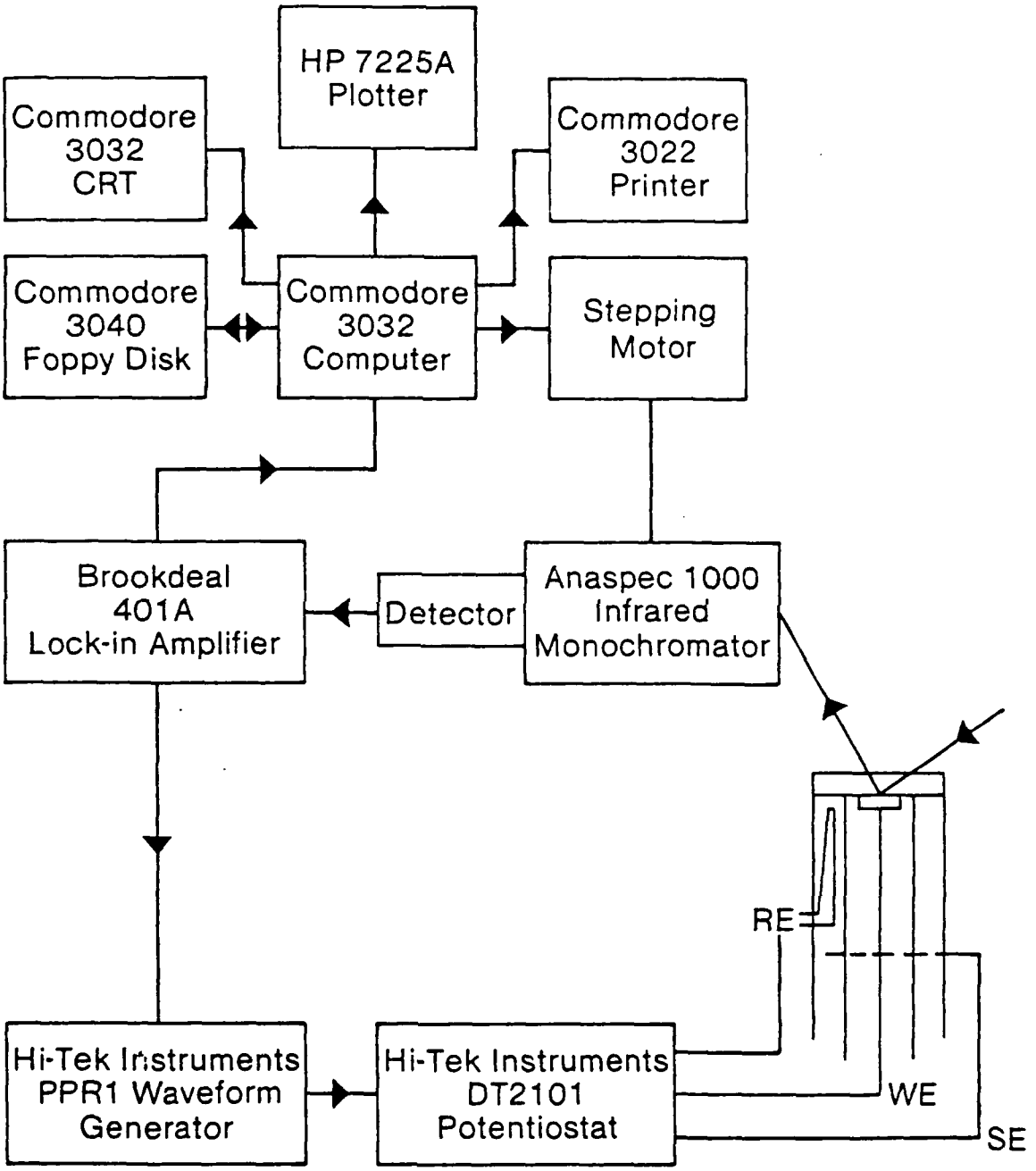
HP 7225A
Plotter
Commodore
3032
CRT
Commodore
3022
Printer
Commodore
3040
Foppy Disk
Commodore
3032
Computer
Stepping
Motor
Brookdeal
401A
Lock-in Amplifier
Detector
Anaspec 1000
Infrared
Monochromator
RE
WE
SE
Hi-Tek Instruments
PPR1 Waveform
Generator
Hi-Tek Instruments
DT2101
Potentiostat

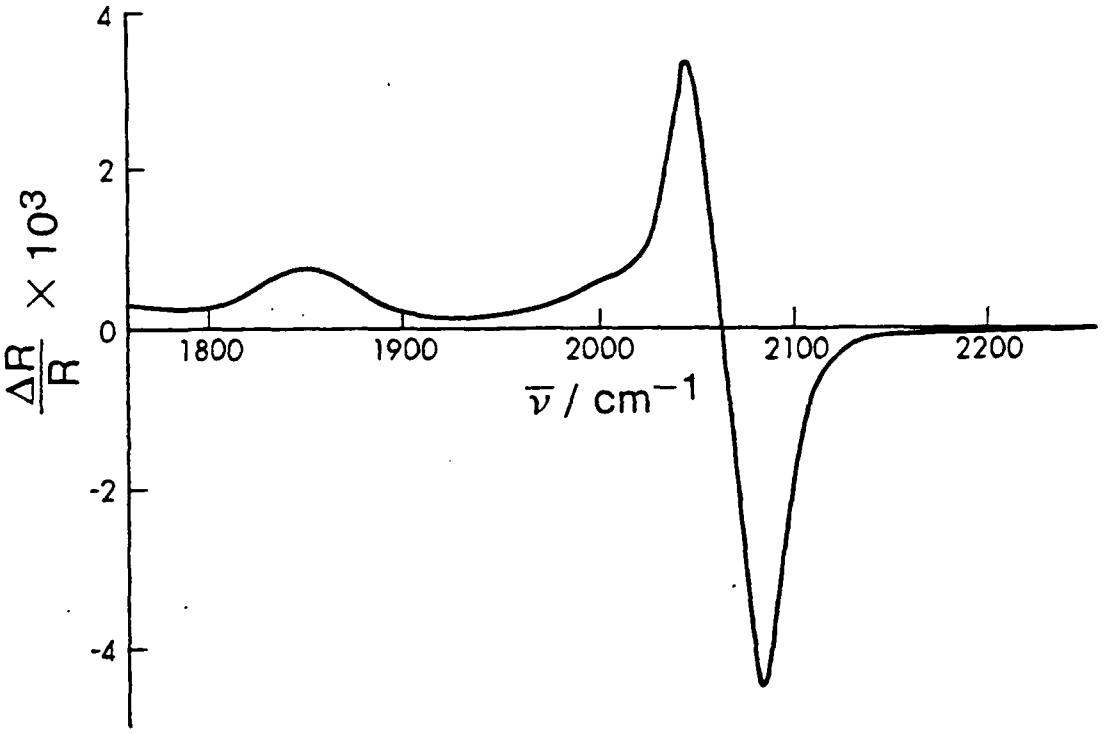
4
2
0
-2
-4
$\frac{\Delta R}{R} \times 10^3$
1800
1900
2000
2100
2200
$\bar{\nu}$ / cm^{-1}

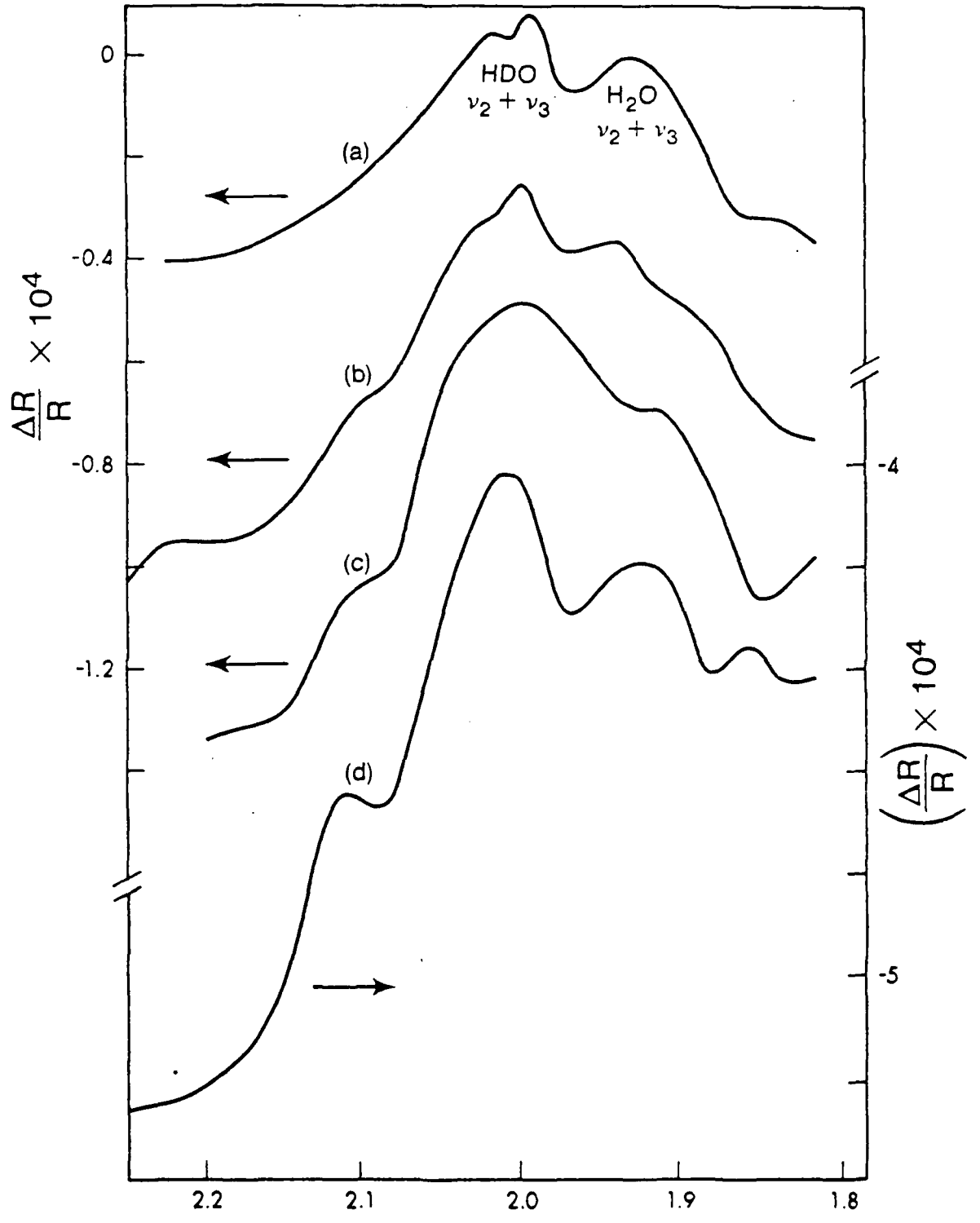
HDO
$\nu_2 + \nu_3$
H_2O
$\nu_2 + \nu_3$
(a)
(b)
(c)
(d)
0
-0.4
-0.8
-1.2
-4
-5
$\frac{\Delta R}{R} \times 10^4$
$\left(\frac{\Delta R}{R}\right) \times 10^4$
2.2
2.1
2.0
1.9
1.8

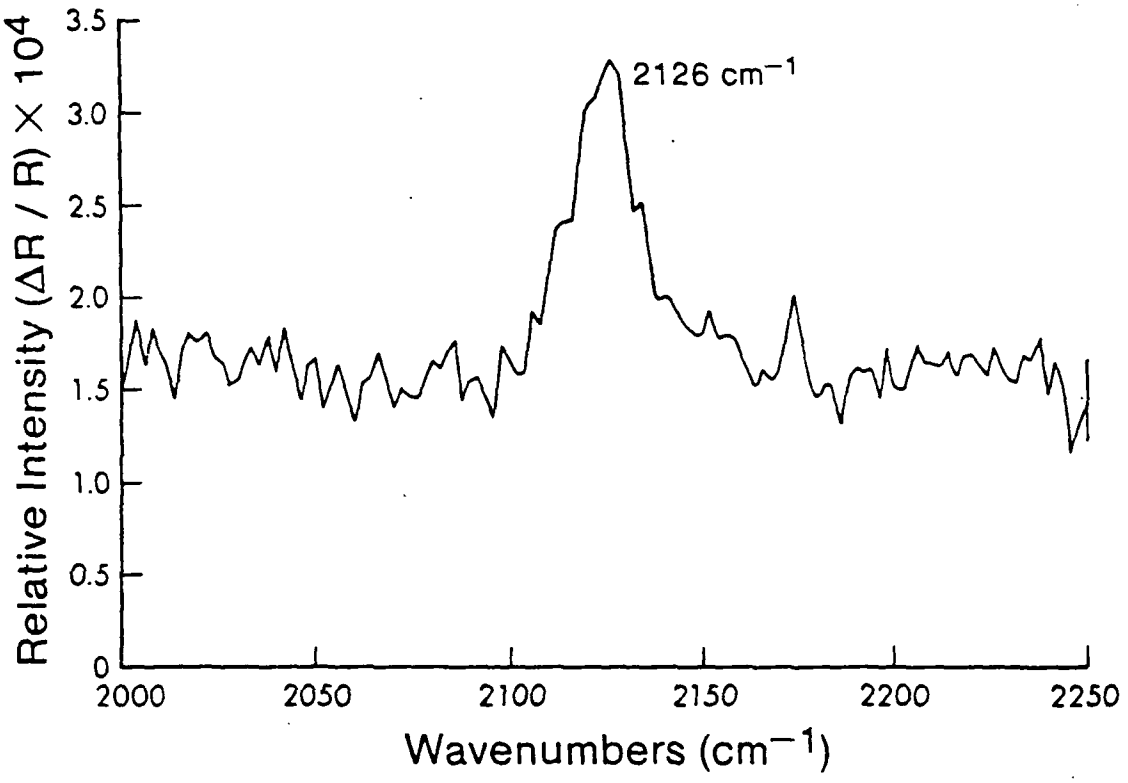
2126 cm^{-1}
Relative Intensity (ΔR / R) × 10^4
3.5
3.0
2.5
2.0
1.5
1.0
0.5
0
2000
2050
2100
2150
2200
2250
Wavenumbers (cm^{-1})

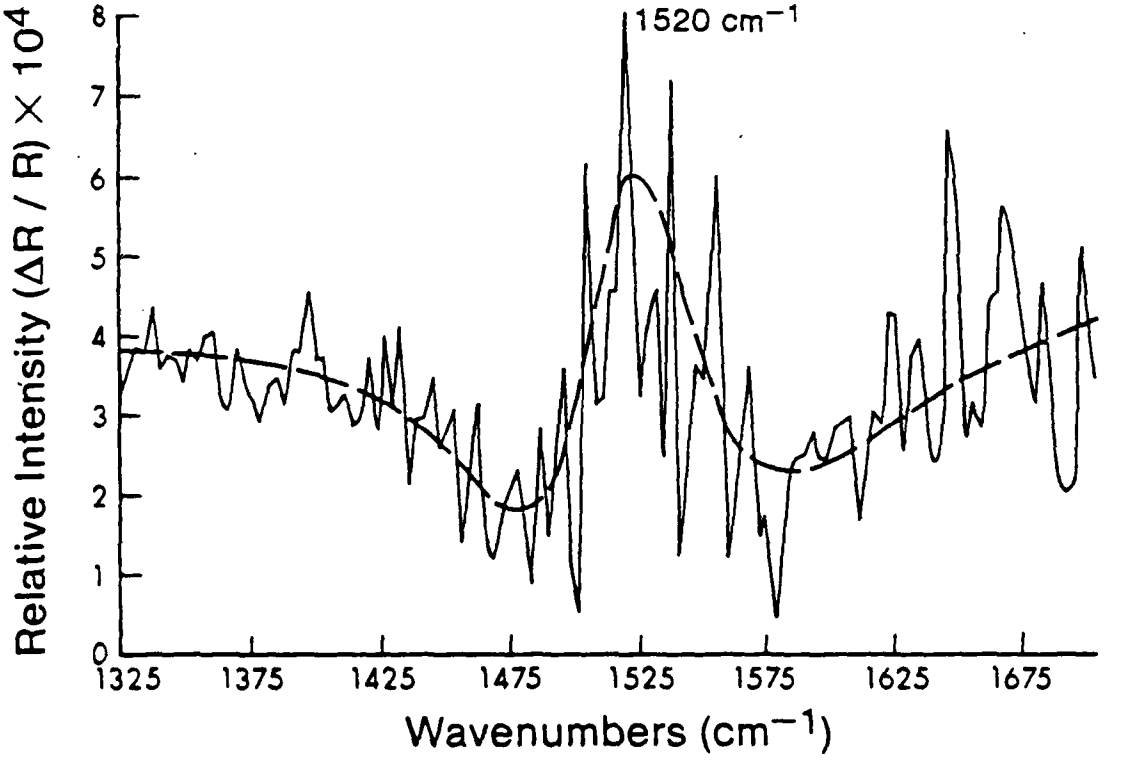
1520 cm^{-1}
Relative Intensity (ΔR / R) × 10^4
8
7
6
5
4
3
2
1
0
1325
1375
1425
1475
1525
1575
1625
1675
Wavenumbers (cm^{-1})

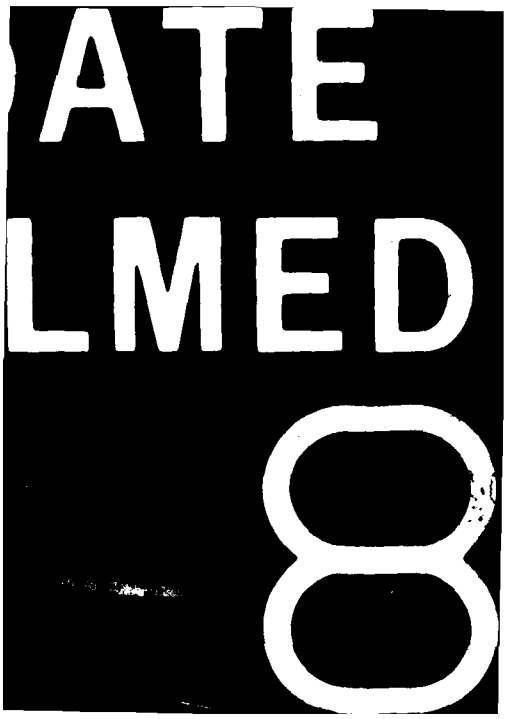
ATE
LMED
8